ANL-6032
Particle Accelerators and
High-Voltage Machines
(TID-4500, 15th Ed.)
AEC Research and
Development Report

ARGONNE NATIONAL LABORATORY
P. O. Box 299
Lemont, Illinois

PARTICLE ACCELERATOR DIVISION

Summary Report

November, 1958 through May, 1959

Albert V. Crewe, Director
John P. FitzPatrick, Associate Director
D. S. Manson, Assistant Director

December, 1959

Previous Summary Reports:

ANL-5630	April 1956 through September 1956
ANL-5713	October 1956 through March 1957
ANL-5803	April 1957 through September 1957
ANL-5864	October 1957 through April 1958
ANL-5956	April 15, 1958 through October 1958

Operated by The University of Chicago
under
Contract W-31-109-eng-38

DISCLAIMER

This report was prepared as an account of work sponsored by an agency of the United States Government. Neither the United States Government nor any agency Thereof, nor any of their employees, makes any warranty, express or implied, or assumes any legal liability or responsibility for the accuracy, completeness, or usefulness of any information, apparatus, product, or process disclosed, or represents that its use would not infringe privately owned rights. Reference herein to any specific commercial product, process, or service by trade name, trademark, manufacturer, or otherwise does not necessarily constitute or imply its endorsement, recommendation, or favoring by the United States Government or any agency thereof. The views and opinions of authors expressed herein do not necessarily state or reflect those of the United States Government or any agency thereof.

DISCLAIMER

Portions of this document may be illegible in electronic image products. Images are produced from the best available original document.

TABLE OF CONTENTS

		Page
I.	Publications	3
II.	Theoretical Studies	8
III.	Model Magnet Studies	10
IV.	Ring Magnet Vacuum Chamber	11
V.	Vacuum Pumping System	18
VI.	Ring Magnet Power Supply	21
VII.	Radio-frequency System	27
VIII.	Injection System	31
IX.	Theoretical Studies on Radial Motion through the Linear Accelerator	36
X.	Miscellaneous	38

PARTICLE ACCELERATOR DIVISION

Summary Report

I. PUBLICATIONS

Abstracts of ANLAD Reports

ANLAD-55 "Helical Quadrupole Magnetic Focusing Systems"
L. C. Teng (February 18, 1959)

A. V. Crewe pointed out that with air core and high field a helical quadrupole magnetic lens is easier to build than a conventional alternating sectional quadrupole focusing magnet system. The motion of a charged particle in such a helical quadrupole field is studied here under the linear paraxial approximation. The result shows that the focusing action of such a helical quadrupole system is about 10% stronger than that of a corresponding alternating sectional system with the same periodicity and field gradient. With appropriately chosen field gradient, pitch and length, a helical quadrupole magnet can be designed to form point images from point sources located on the axis. Formulas and graphs relating these parameters are derived.

An example of a helical quadrupole lens system is shown. In the analogous case of alternating conventional lenses, within a distance λ, the pitch of the helix, there would normally occur two pairs of focus-defocus elements.

ANLAD-56 "Energy Spread from the Linear Accelerator"
John R. Hiskes (on summer appointment to ANL from The University of California Lawrence Radiation Laboratory) (March 25, 1959)

Proton phase motions for the Argonne 50-Mev injector Linac have been calculated with the Argonne "George" computer. The fundamental equation is nonlinear. A number of phenomena have been investigated and results examined via figures in phase space; in particular, output phase and energy spreads have been investigated as a function of random gradient fluctuations and general gradient "tipping." Sets of random gradient fluctuations were chosen from a uniform distribution between -2% and +2%, -4% and +4%, and -8% and +8%. Taking into account post-Linac debunching (energy spreads of 400 kev are allowed before the debuncher), no disturbing effects were seen. For space fluctuations only protons can have their mean output energy shifted by 500 kilovolts, but spreads do not exceed 400 kilovolts for the worst (8%) case. With time fluctuations the energy spread in the latter case may become seriously large. A "tipping" of 10% end-to-end indicates an induced output energy spread somewhat greater than 400 kilovolts.

Internal Memoranda

K. Burba

KB-7 1200-kw M-G Set Inspection and Tests at Westinghouse Electric Corporation (September 29, 1958)

G. O. Calabrese

*EFF-GOC-AAG-1 Preliminary Ring Magnet Power Calculations (Rev. February 24, 1959)

D. Cohen

DC-2 Quadrupole Magnet Forces (February 4, 1959)

DC-3 Review of Some Concepts Involved in ZGS Injection (March 11, 1959)

H. Fechter

*HF-MS-1 Electrolytic Tank Construction, Calibration and Applications (October 13, 1958)

E. F. Frisby

*EFF-GOC-AAG-1 Preliminary Ring Magnet Power Calculations (Rev. February 24, 1959)

R. George

RG-1 Re-optimizing in New Symbolic Expressions (February 10, 1959)

H. Kampf

HAK-7 Tuning Error Effects Upon Phase and Amplitude Characteristics of the Accelerating Gap Voltage (January 27, 1959)

F. Markley

*FWM-RDR-1 Specifications for Bonding Material and Its Use for the Prototype Magnet Block (April 24, 1959)

---

*Indicates joint authorship

J. Martin

JHM-4	Trip Report to AERE, CERN, Delft, Philips, Saclay and Hamburg (January 15, 1959)
JHM-5	Synchrotron Beam Control by RF Manipulator (May 18, 1959)

J. Mech

JFM-7	Relays for Control and Interlocking (September 8, 1958)
JFM-8	Design for Pulsing Generators (December 23, 1958)
JFM-9	Linac Vacuum System Interlocking - I (March 27, 1959)
JFM-10	Linac Vacuum System Interlocking - II (April 13, 1959)
JFM-11	Linac Cavity Tuning and Monitoring (May 22, 1959)

J. Moenich

JSM-4	Conductance and Tolerable Gas Loads - Ring Vacuum Chamber Octants (January 19, 1959)
JSM-5	Experimental Epoxy Fiberglass-coated Vacuum Chamber (Dwb. No. 06-301-5 - Behavior under Vacuum) (April 7, 1959)

T. H. McGreer

THMcG-2	Generator Speed Control (August 18, 1958)

D. E. McMillan

DEM-2	Preliminary Considerations Regarding the ZGS Control and Interlock System (October 24, 1958)

R. Roman

*FWM-RDR-1	Specifications for Bonding Material and Its Use for the Prototype Magnet Block (April 23, 1959)

*Indicates joint authorship

R. Rothe

RER-1	Magnetic Characteristics of Ferrites (December 12, 1958)
RER-2	Electromagnetic Properties of the Empty Model RF Accelerating Cavity (May 15, 1959)

D. Shirer

DLS-1	ZGS Frequency Program, Energy and Equilibrium Orbit Parameters as a Function of Guide Fields (August 22, 1958)

M. Striegl

*HF-MS-1	Electrolytic Tank Construction, Calibration and Applications (October 13, 1958)

L. C. Teng

*EAC-LCT-2	New "Frozen" Parameters of the ZGS (December 16, 1958)

R. Trcka

*RT-WDZ-1	Alkali-Aggregate Reaction in Concrete (March 12, 1959)

W. D. Zander

*RT-WDZ-1	Alkali-Aggregate Reaction in Concrete (March 12, 1959)

A. V. Crewe, R. H. Hildebrand, U. E. Kruse, S. C. Wright, C. M. York

CHKWY-7	Shielding Considerations for the Control Room and Linear Accelerator Building (January, 1959)
KWY-1	An Estimate of the Amounts of Liquid Hydrogen and Liquid Nitrogen Required by the Experimental Program of ZGS (February 12, 1959)

*Indicates joint authorship

External Publications

Helical Quadrupole Magnetic Focusing Systems
Lee C. Teng
American Physical Society Meeting, Washington, D. C., April 30-May 2, 1959

A Bias Function Generator for the ZGS
L. K. Wadhwa
IRE Transactions on Nuclear Science NS-6, 2-10 (March, 1959)

II. THEORETICAL STUDIES

E. A. Crosbie, L. C. Teng

A. Motion of Charged Particles in a Linear Helical Quadrupole Magnet

This study, which was first reported in the last summary report (ANL-5956), was continued. It was found that the analog computing machine could not give the desired accuracy. On closer examination it was realized that by a special transformation the orbit equations can be brought into a form which is analytically soluble in terms of transcendental functions. The focusing properties of these helical quadrupole magnet systems of infinite or finite lengths are, then, derivable through the solution of a set of algebraic equations. This was carried out with the help of IBM-704 computing machines. The numerical results and the analytical developments are given in ANLAD-55.

B. Study of the $2\nu_z - \nu_x = 1$ Resonance

Continued effort of studying this resonance with computing machines indicated only that the effect of coupling between the radial and the vertical oscillations due to this resonance in the ZGS is very small. It is, perhaps, more fruitful to seek a new attack on this problem. The orbit equations with the relevant nonlinear terms can be studied analytically by various approximation methods. These methods should give, at least, an order of magnitude estimate on the resonance effect.

C. ZGS Orbit Studies

In order to investigate the general incorporated effects of the soft fringing field at the main guide magnet (octant) edge (end) and the field in the DC magnet, a computing program for the "George" digital computer is being written. The immediate problem to be solved by this program is a more precise design for the DC magnets than that obtained by linear calculations using infinitely hard field edges.

For this program the field of the guide magnets is assumed to be spatially uniform except near the edges. The fringing field there is specified on the median plane to be approximately the same as that given by measurements on experimental model magnets. The magnetic field of the DC magnets is also specified on the median plane. The field away from the median plane is given by Maxwell equations in the form of a power series expansion in the vertical coordinate. The magnitude and radial variation of the DC field are, then, adjusted to give the desired orbital motion for the protons during injection. It is planned to incorporate "errors" into the guide magnetic field at a future date.

The orbits are computed in the following manner. In straight sections where the field is zero and inside the guide magnets where the field is uniform the orbit equations are analytically integrable. The changes in the orbit coordinates (positions and slopes) across these regions can, therefore, be obtained by appropriate one-step transformations. In the fringing fields of the guide magnet edges and the fields of the DC magnets where the orbit equations are not analytically integrable, numerical integration is employed. Provisions are made to start the particle at any point around the machine and to print out the orbit coordinates at an adequate number of somewhat adjustable azimuthal locations.

D. Arbitrary Function Fitting Code

To fit the measured edge field of the guide magnet by given function forms, we have developed a Fortran IBM program. This program will give the best least-square fit to a series of up to 100 points with a general function having up to 20 parameters. For a given functional form it is only necessary to write the Fortran subroutines for calculating the function with the given form and insert these subroutines into the main program.

E. Fringing Field at an Ideal Two-dimensional Magnet Edge

The conformal mapping giving the fringing field at an ideal (permeability of iron = ∞) two-dimensional simple magnet edge was carried out in detail. The result was plotted to supply a comparison with the fringing field assumed for ZGS orbit calculations.

F. Variable-energy, Multi-particle Isochronous Cyclotrons

Because of the growing interest in the Laboratory in this type of sectorial cyclotron, a general study was made on the magnetic field and RF requirements for given ranges of types of ions and energies. In particular, the RF frequency range, the range of flutter and spiral angle of the magnetic field, and the power requirements were plotted. This study was then applied to give a comparison of the ORIC (Oak Ridge Isochronous Cyclotron) and a similar sectorial cyclotron, with 100-in. pole diameter.

G. Controls and Timing of ZGS

A first crack was made at incorporating and presenting systematically and logically the various controls (automatic and manual) and adjustments required, the firing order of the components, the timing intervals and their tolerances for the ZGS. Rough general charts were drawn to serve as a starting point for further detailed considerations and studies.

III. MODEL MAGNET STUDIES

Martyn Foss

Results obtained with a $\frac{1}{7}$-scale straight model made of hot-rolled rimmed steel diluted with 2.5% insulation indicate that there will be no trouble obtaining an external beam at 12.5 Bev. Work is proceeding satisfactorily on the program to determine the size and location of the correcting holes in the yoke.

A pulsed model magnet program was initiated and studies are being made of eddy current and hysteresis effects.

A $\frac{1}{7}$-scale curved model is being constructed for pulsed work and is nearing completion.

IV. RING MAGNET VACUUM CHAMBER

W. B. Hanson, F. W. Markley

The design and testing of the double wall vacuum chamber system has reached advanced stages during the last few months. The design of inner vacuum chambers has narrowed down to two specific methods of construction.

A. Inner Vacuum Chamber

1. Epoxy Chamber

This design consists of 6-in. parallel rings of stainless steel, $\frac{1}{32}$-in. thick, bonded together with thin 2-in. overlapping rings of stainless steel. The remainder of $\frac{1}{8}$-in. wall thickness is built up of epoxy resin and glass cloth using vacuum bag techniques. Under a contract, Convair Division of General Dynamics Corporation developed a method of fabrication and has built a 3-ft prototype chamber. Vacuum tests on this chamber are now being performed.

This chamber is formed in two halves and later assembled by an "H" strip along each side (see Fig. 1). All bonding and laminating, except the final bonding of the two halves, is done under heat and pressure.

The sequence of fabrication is as follows:

a. Form 6-in. and 2-in. stainless steel bands into half rings.
b. Lay up on a heated mandrel the 6-in. bands with approximately $\frac{1}{8}$-in. space in between each.
c. Lay up 2-in. steel band overlapping joints with Minnesota Mining and Manufacturing Company AF-31 bonding tape in between the layers of steel. The tape must serve three functions:

   (1) produce a structurally strong joint;
   (2) insulate steel bands from one another electrically to minimize eddy current effects; and
   (3) provide a vacuum-tight joint.

d. Vacuum bag cure bonded joints on the heated mandrel with a step cure cycle going to 350° F.
e. Check for electric shorts from band to band.
f. Coat inside surface with epoxy resin mold release agent.

g. Lay up wall in layers of glass cloth and epoxy resin to a total thickness of $\frac{1}{8}$ in.
h. Vacuum bag cure epoxy at 330°F.
i. Remove from mandrel and thoroughly clean inside high vacuum surface so that outgassing will be minimized.
j. Bond "H" strip to one-half section using low-cure temperature epoxy resin.
k. Clean off excess epoxy resin.
l. Join and bond two halves using care not to squeeze out excessive resin, since mechanical cleaning after this operation is not possible.
m. Weld flanges on protruding stainless steel of end bands.
n. Complete bond at side strip where heat of welding has affected epoxy.
o. Finish machine flange.
p. Check for and repair any vacuum leaks.

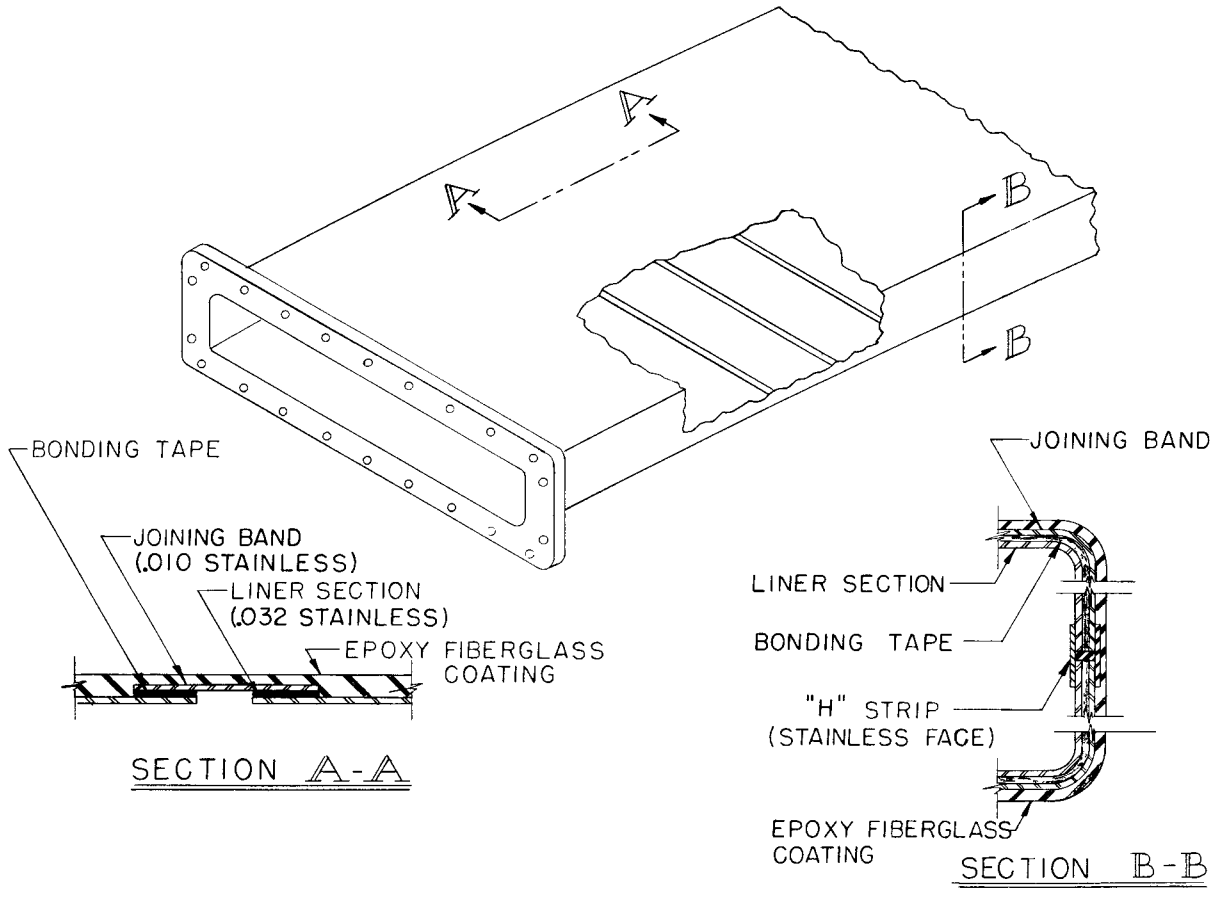

EPOXY CHAMBER

FIG. 1

From a construction aspect, this design is economical and basically very sound. Only relatively minor problems occurred during fabrication of the prototype chamber by Convair, and these were readily corrected.

From the standpoint of vacuum characteristics and radiation degradation, the epoxy chamber has some definite disadvantages. To overcome these disadvantages, we are working on an alternate design of chamber using a product known as "Spacemetal."

2. "Spacemetal" Chamber

The "Spacemetal" chamber incorporates the use of a stainless steel sandwich made up of two outer skins with a corrugated core metal between. This material was developed by North American Aviation Company under an Air Force contract.

This chamber is fabricated by nesting together 6-in. wide box sections (see Fig. 2). The flat "Spacemetal" is cut to shape and bent around an accurate heated mandrel. An outer clamping device provides the pressure for cure.

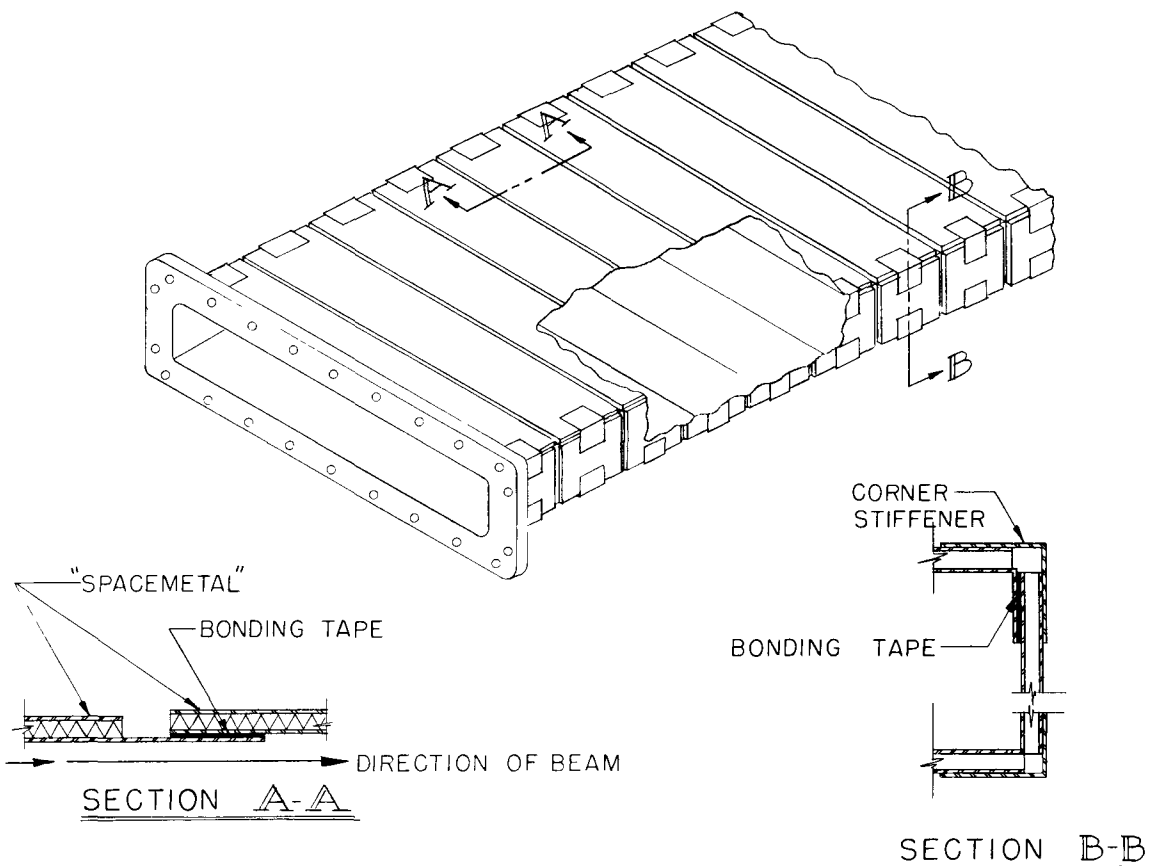

"SPACEMETAL" CHAMBER

FIG. 2

The advantages which the "Spacemetal" chamber offers are the following:

a. Plastic outgassing is less than $\frac{1}{2}$ that of the epoxy chamber.
b. Effects of high-energy radiation degradation are expected to be small by comparison with that anticipated for the epoxy chamber. The stress level in the plastic portion of the chamber is very small and the overlapping joints are in the direction of the beam, offering improved shielding to the bonded joint.
c. The relative stiffness of this chamber is about twice that of the epoxy chamber and, furthermore, does not depend on epoxy for its strength. The chief function of the bonding material is to provide a vacuum seal and insulate each section electrically.
d. The eddy current effect on the magnetic field is about $\frac{1}{2}$ that of the epoxy chamber.

B. Rough Vacuum Chamber

The rough vacuum chamber is a composite of the upper and lower magnet poles forming the top and bottom walls, and a gasketed plank on either side forming the side walls (see Fig. 3).

Vacuum sealing of the magnet poles is accomplished by:

1. plate-to-plate seal formed by bonding the magnet plates using an epoxy impregnated fiber glass;
2. finished magnet blocks will be vacuum checked and any leaks repaired;
3. it may be desirable to gain additional vacuum insurance by bonding a cured epoxy Fiberglas laminate to the pole face;
4. block-to-block seal is formed by the use of compressible rubber flat gasket bonded in place using epoxy resin; and
5. a sealing surface for the side-wall gasket is formed by running an azimuthal plastic strip bonded to the upper magnet pole face.

The side walls are bonded to the lower magnet pole face after the coil is installed. The complete seal is formed with the lowering of the upper magnet pole on to the gasketed side walls and the bolting of the flanged transition box against the "T" gasketed end faces (see Fig. 3).

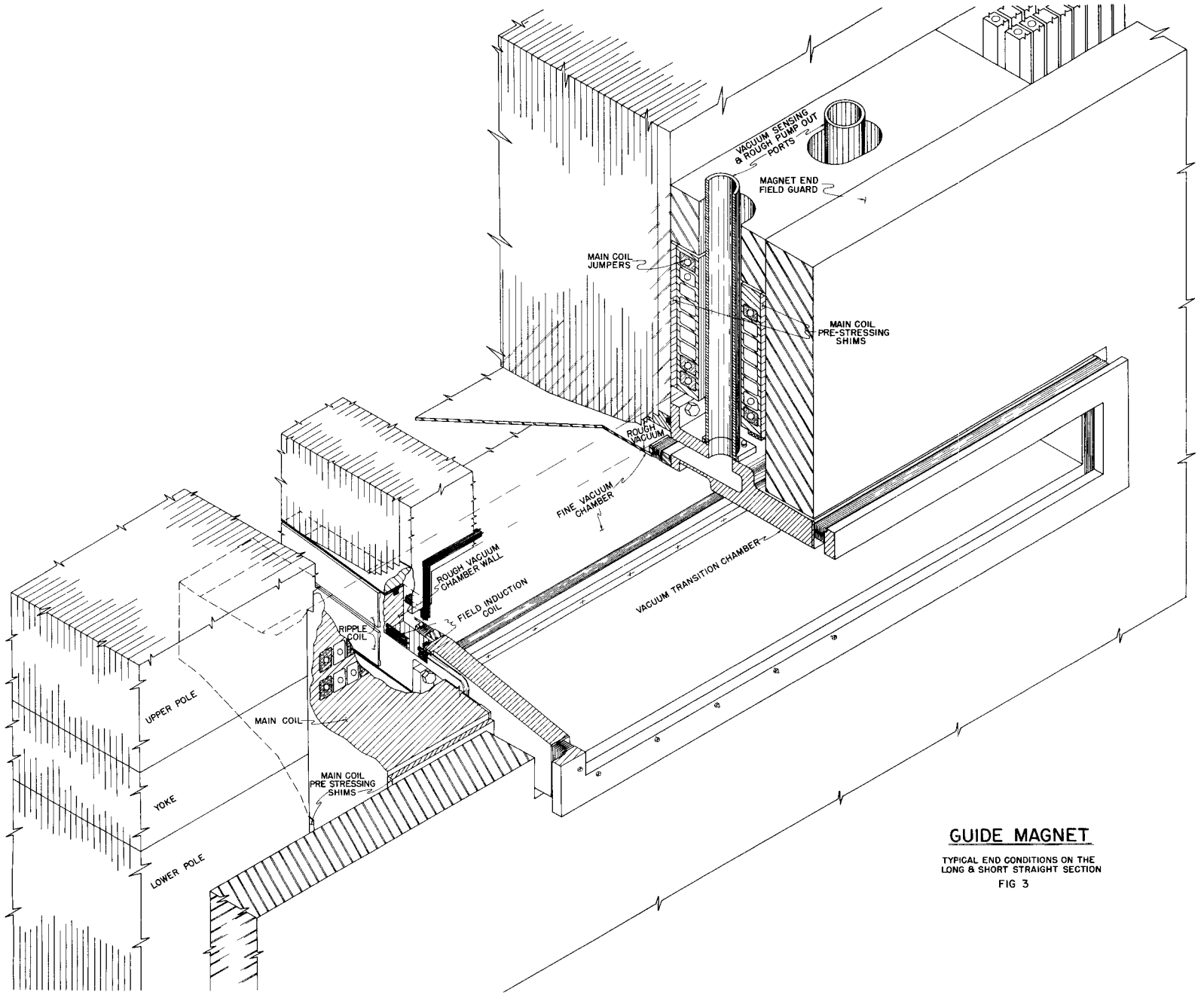

GUIDE MAGNET

TYPICAL END CONDITIONS ON THE LONG & SHORT STRAIGHT SECTION

FIG 3

A testing program to check out these principles is being carried out in our plastics laboratory by F. W. Markley and R. D. Roman.

C. Rough Vacuum Chamber Test Program

Four magnet blocks, $\frac{1}{4}$-scale in all dimensions except for plate thickness, which is full scale, have been built. These blocks were constructed by a new method developed since the last report (ANL-5956). The interlaminar insulation used is an uncured, epoxy-impregnated system of parallel glass fiber reinforcing strands (MMM's Scotchply XP-141, 50% Resin). The blocks were built using a joint by joint cure rather than a stack cure as described previously (ANL-5956). Each lamination was bonded in place with heat and pressure prior to the addition of the next lamination. The laminating procedure is as follows:

1. Remove scale from cold-rolled plates. (Ground or milled plates need no treatment.)
2. Degrease in trichlorethylene vapor degreaser.
3. Apply Scotchply XP-141 to one side of hot plate.
4. Insert the plate in a hydraulic press with a heated movable platen with the Scotchply-covered side facing the previously laid-up section.
5. Close the press and cure for 5 min. at joint pressure of 30 ± 5 psi and joint temperature of 335 ± 5° F.
6. At the end of the cure cycle check for shorts across joint using a 110-volt tester. If short, remove the last plate.
7. Open press and repeat cycle until 92 laminations have been bonded together.

Internal memorandum FWM-RDR-1 gives detailed instructions for the complete process.

The $\frac{1}{4}$-scale blocks produced by the above procedure were short-free and strong (200-3000 psi block shear). Total layup time was 12 min per lamination and the stacking factor was better than 98%. The blocks were not vacuum tight. This was due to uneven curing pressure caused by thermal bowing of the platen in the press used. The layup method is very satisfactory and will be used to produce a full-scale magnet block. The contract for the construction of this block was awarded to the Blaw-Knox Company, Foundry and Mill Machinery Division.

The four $\frac{1}{4}$-scale blocks have been made vacuum tight by facing the pole surface with a cured epoxy Fiberglas laminate. The blocks are to be used in the assembly of a rough vacuum chamber similar to the proposed final chamber (see Fig. 4). The vacuum cavity thus formed will be $\frac{1}{4}$ scale in the horizontal dimension and full scale in the vertical dimension, and is to be used in checking the proposed gasket system described above.

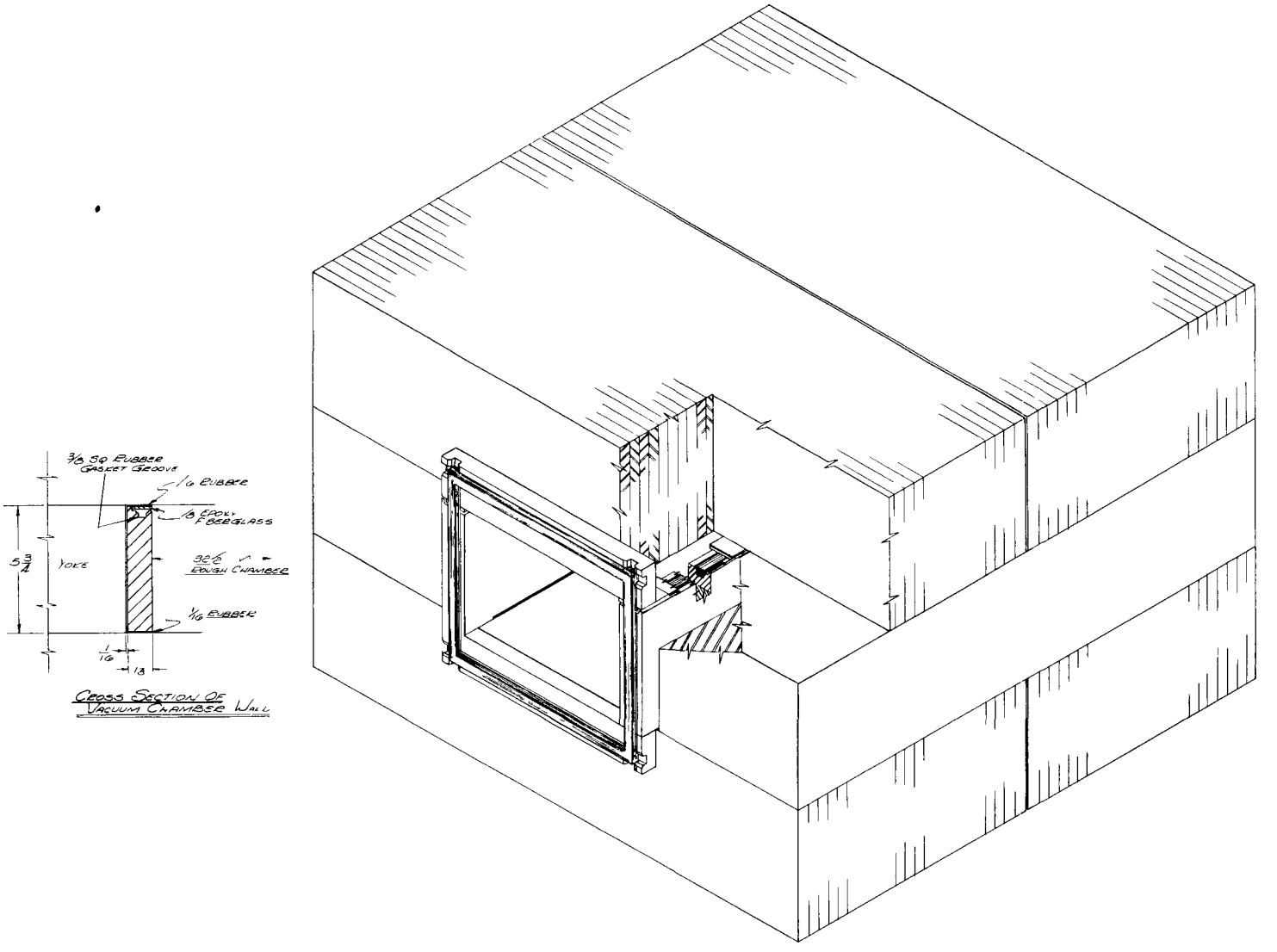

ROUGH VACUUM CHAMBER TEST SETUP

FIGURE 4

V. VACUUM PUMPING SYSTEM

R. Trcka, J. Moenich

As a result of the preliminary studies and design of several vacuum pumping systems, the schematic piping diagram, as shown in Fig. 5, is to be used as a basis of final design and represents a typical installation of pumping equipment and piping for the vacuum system for each of the eight straight sections.

The vacuum system consists of an 8-in. finishing line that is to be used as a combination finishing, backing and holding line for the oil diffusion pumps and installed as a closed ring manifold in the ring tunnel building. A 6-in. roughing line is also installed as a closed ring manifold in the tunnel and serves as a rough vacuum line for pumping on the outer vacuum chamber of an octant. Each straight section contains two rough vacuum connections at each magnet end for the magnet outer vacuum chamber, two vacuum chamber rectangular gate valves for isolating portions of the ring magnet vacuum chamber, two roughing connections at the bottom of the straight section, two 32-in. diameter high-vacuum pumping connections also in the bottom of the straight section, two 32-in. pneumatically operated gate valves, two Freon-cooled combination low-temperature and -20° F baffles connected to one refrigeration condensing unit, two 32-in. oil fractionating diffusion pumps, one 1000-cfm Roots-type mechanical booster pump, and two 130-cfm mechanical vacuum pumps with oil traps.

The following requirements were considered in the selection of the vacuum pumping system as shown:

A. Locate the mechanical rough vacuum pumps in the ring tunnel building in the vicinity of the straight sections for the purpose of making the connected piping as short as possible.
B. Provide a differential pumping system in each magnet sector.
C. All high-vacuum pumping connections to be located in the bottom of the straight sections.
D. Use Roots-type mechanical booster pumps as an intermediate pump for roughing the ring magnet vacuum chamber and backing the diffusion pumps at period of high mass flow.
E. Provide a pumping system with sufficient flexibility of operation and reliability to conform to accelerator operation.

The location of the mechanical pumps in the ring tunnel building in conjunction with the roughing and finishing closed ring manifold piping is advantageous from the standpoint of eliminating long runs of connected piping, and positions the pumps in the close proximity of the high-vacuum pumps for improved pumping efficiency. The mechanical pumping arrangement with its associated piping lends itself readily to packaging the Roots-type booster pump and the two mechanical pumps as a single compact unit

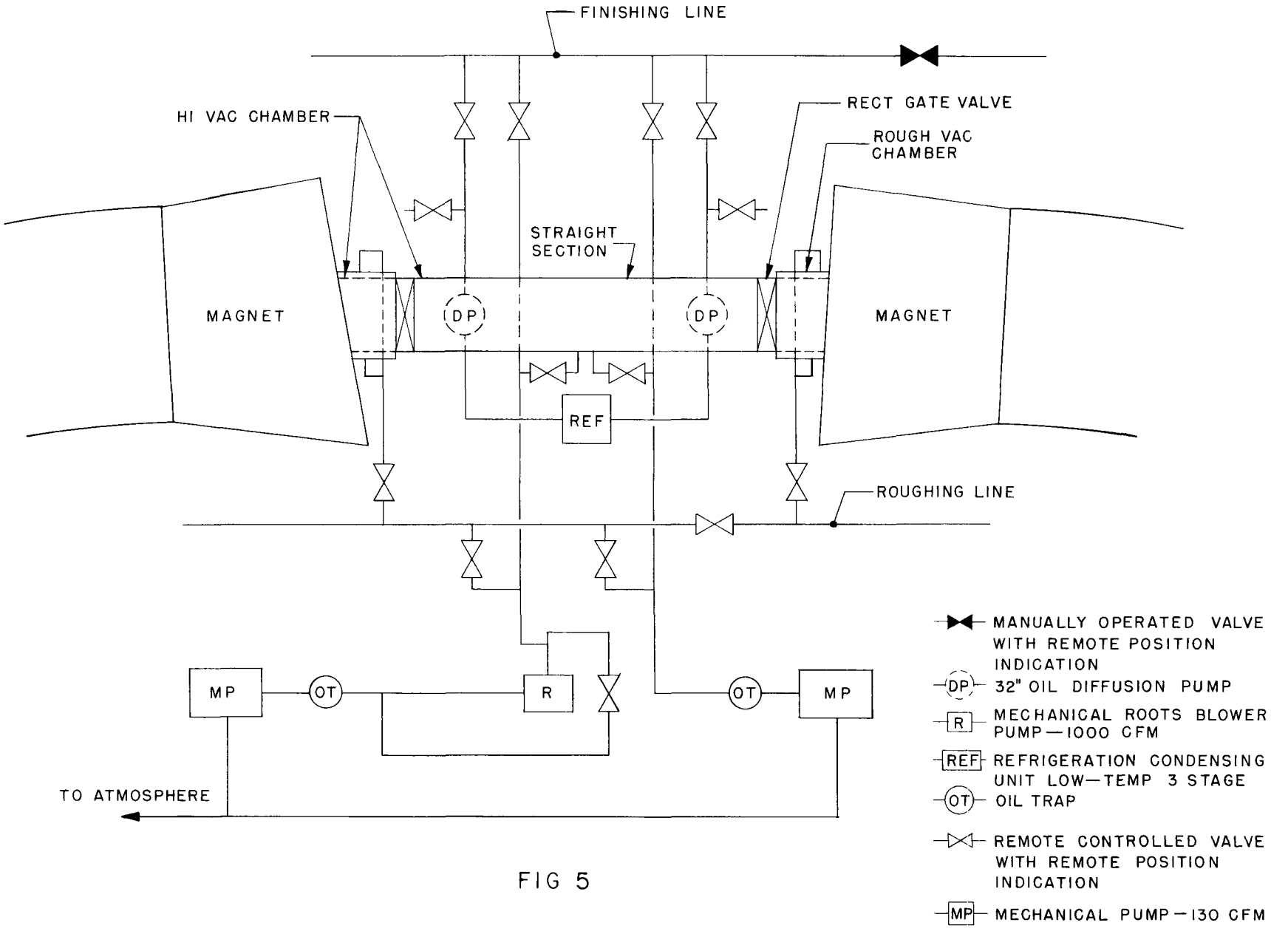
FINISHING LINE
HI VAC CHAMBER
RECT GATE VALVE
ROUGH VAC CHAMBER
STRAIGHT SECTION
MAGNET
DP
DP
MAGNET
REF
ROUGHING LINE
MP
OT
R
OT
MP
TO ATMOSPHERE
MANUALLY OPERATED VALVE WITH REMOTE POSITION INDICATION
DP 32" OIL DIFFUSION PUMP
R MECHANICAL ROOTS BLOWER PUMP—1000 CFM
REF REFRIGERATION CONDENSING UNIT LOW—TEMP 3 STAGE
OT OIL TRAP
REMOTE CONTROLLED VALVE WITH REMOTE POSITION INDICATION
MP MECHANICAL PUMP—130 CFM

FIG 5

for conservation of floor space, and, if necessary, ability to remove the entire unit in a short period of time for maintenance and repair by replacing it with a spare package unit.

The use of Roots-type mechanical booster pumps is advantageous in that they can be used to rough the entire system from a pressure of 20 mm Hg to an operating foreline pressure for the diffusion pumps in a shorter period of time than can be expected when using mechanical pumps alone. In addition, the booster pumps are utilized for backing the diffusion pumps during period of high gas throughput. During this period of high mass flow, backstreaming of oil from the diffusion pumps to the baffles will occur, and it is desirable to prevent this tendency by using high-capacity backing pumps to maintain a foreline pressure within tolerable limits.

The valving arrangement at each straight section enables the vacuum system to be flexible to the extent that the roughing pumps can be used interchangeably as roughing, backing or holding pumps. The Roots-type booster pump can be used as a roughing or backing pump, and can be shut off and isolated in the system on standby at high vacuum. Any straight section can be opened to atmosphere while the remainder of the diffusion pumps continue to pump, and the two diffusion pumps on the opened straight section are also held by the backing and holding pumps connected commonly to the closed ring manifold.

The individual connection of the high-vacuum pumps to the closed ring manifold and the manifold in turn serving as a common header to the mechanical pumps of all the straight sections permits a malfunction or complete loss of several mechanical pumps when operating at high vacuum without requiring the entire vacuum system to be shut down, thereby enabling continued accelerator operation until a designated maintenance period can be utilized for adjusting or repairing vacuum equipment.

VI. RING MAGNET POWER SUPPLY

G. O. Calabrese, E. F. Frisby

Further discussions of the various aspects of the ring magnet power supply were held with the three manufacturers interested in bidding for the same. Work on the specifications was continued, culminating in S and P Technical Report TR-105-F, Title I, in its preliminary form, dated February 17, 1959, and in the final form, dated April 10, 1959. The final version of the specifications is in process of preparation and will be issued sometime during the first half of July.

Rectifier Connections and Loading

From the discussions held at various times with the three manufacturers above referred to, it appears that three schemes of rectifier connections are considered at each of the four points of supply in the ring magnet, namely:

Manufacturer A: double way rectification, as shown in Fig. 6
Manufacturer B: one way rectification, as shown in Fig. 7
Manufacturer C_1: one way rectification - parallel series scheme, as shown in Fig. 8.

In the design of the power supply we are emphasizing 1) reliability of the equipment, and 2) the fact that the voltages injected at the four points of supply should be exact duplicates of one another. Thus it has appeared highly desirable to analyze the three schemes of connections from the two viewpoints above. Since the loading of the rectifiers affects their reliable operation, we have studied the rectifier loading with the three proposed schemes of connection.

Mercury-arc rectifiers, like other electronic tubes, have a maximum instantaneous voltage and a maximum instantaneous current which cannot be exceeded. In addition, among other factors, their capacity is limited by the ability of the tube to dissipate losses, an ability which is usually described in terms of the average current.

A given mercury-arc rectifier may be operated over a range of voltages; however, the average current decreases as the voltage increases and vice versa. On the basis of accelerated tests, the manufacturer determines the so-called assigned rating. This is such that if the rectifier is loaded at the assigned rating, under the specified temperature conditions, reliable operation will result with low arc-back rate and long life.

The relationship between the DC voltage and the average DC current per rectifier is of the form

$$E/E_1 = (I_1/I)^n \quad ,$$

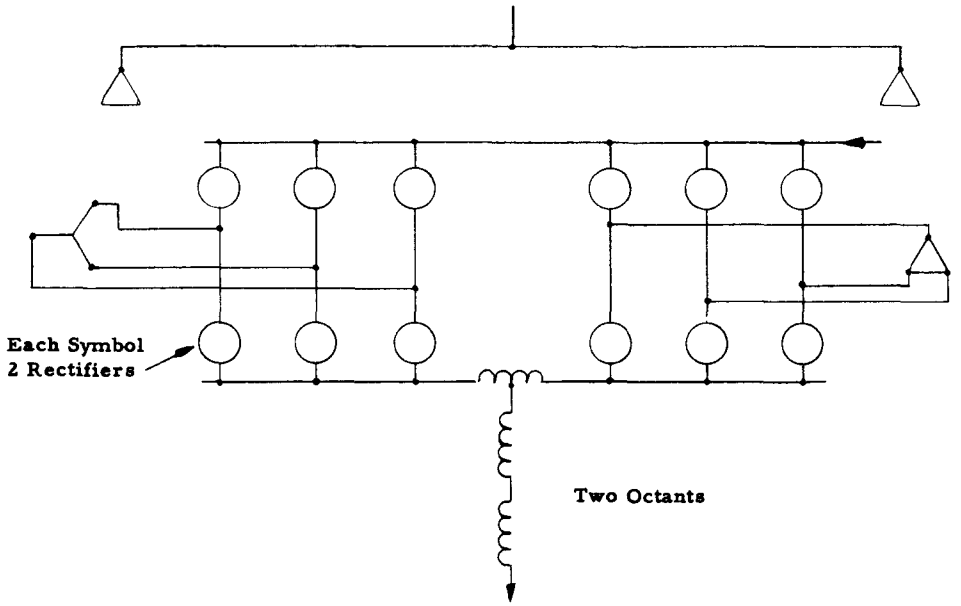

Figure 6

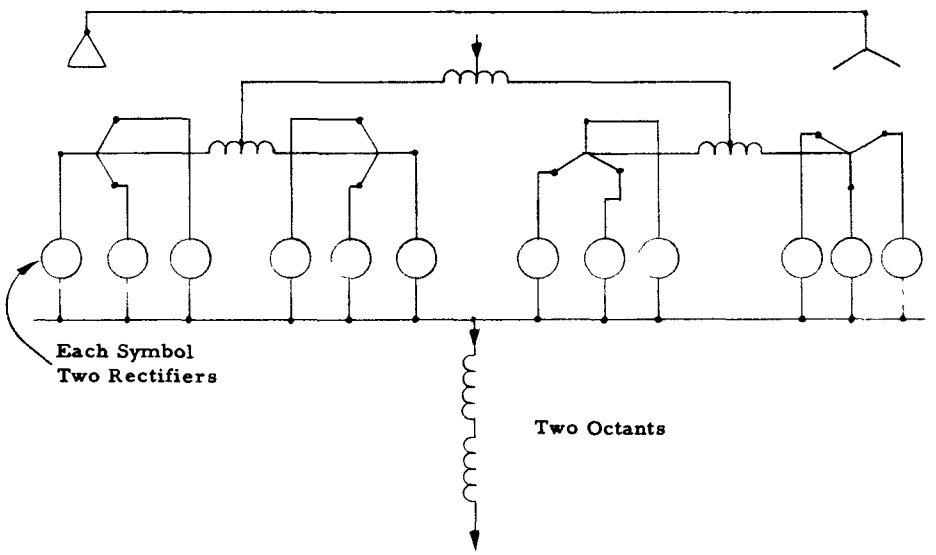

Figure 7

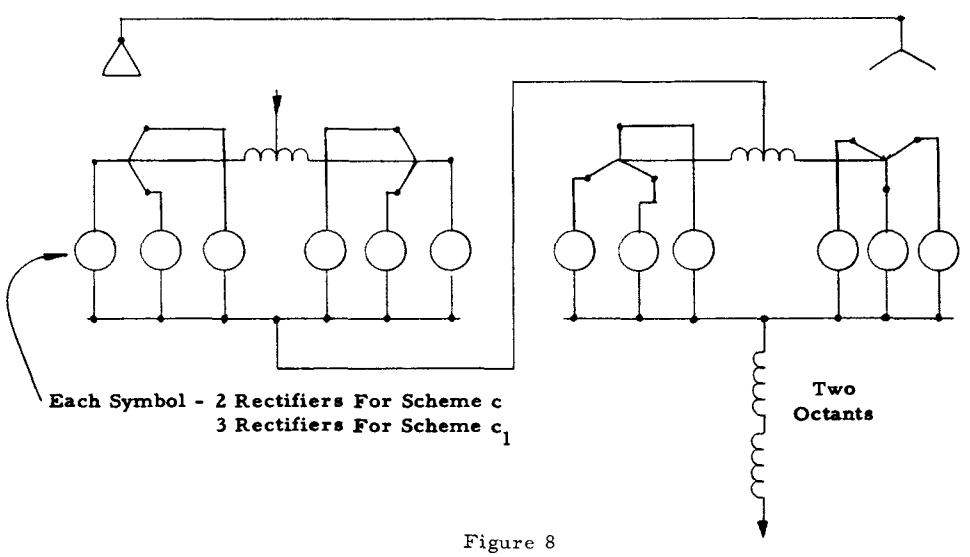

Figure 8

where E and I, and E_1 and I_1 are corresponding values of DC voltage and average current. Here n is an exponent close to 1.0 for some tubes and greater than 1 for others.

The assigned ratings of the rectifiers, as obtained on a preliminary basis from the three manufacturers referred to above, are shown in Fig. 9, in which there are shown the assigned ratings, DC voltage vs. average current, with zero phase-angle control of:

A. Manufacturer A: 16-in. double grid pumpless rectifier with 50° C cooling water inlet temperature;
B. Manufacturer B: 15-in. double grid pumped with 45° C cooling water outlet temperature; and
C. Manufacturer C_1: 16-in. double grid pumped excitron.

Table I gives the assigned rated average current, I_r, corresponding to the values of V_1, the voltage across each rectifier tube, at the beginning and at the end of the rising period of the pulse of the ZGS. In columns 12, 13, 14 are shown the rectifier loadings in per cent of the assigned ratings I_r for the three connections of Figs. 6, 7, 8, respectively. The figures of Table I are based on the pulse shape of Fig. 10 with

$t_1 = t_1' = 1.0$ sec

$T = 4.0$ sec

and

$\Delta t = 0$ or 0.2 sec, respectively, as shown.

The per cent figures of columns 12, 13, 14 permit us to evaluate the relative severity of loading duty imposed on the rectifiers with respect to the assigned ratings, under the different schemes and proposed number of rectifiers.

The mercury-arc rectifier is essentially a switching device. Failure of this switching action results in arc-back. An arc-back is the failure of the rectifying action, due to the formation of a cathode spot on the anode, when the latter is negative with respect to the cathode, which results in a flow of current in the reverse direction, from cathode to anode. The relative degree of reliability from the standpoint of arc-backs of various schemes of operation can be obtained by calculating the probabilities of arc-back. We have started the calculation of the arc-back probabilities which may be expected with the three schemes of Figs. 6, 7, and 8 under the methods of operation presently contemplated.

For comparative purposes, Table II gives a partial list of rectifier data of some existing or projected accelerators.

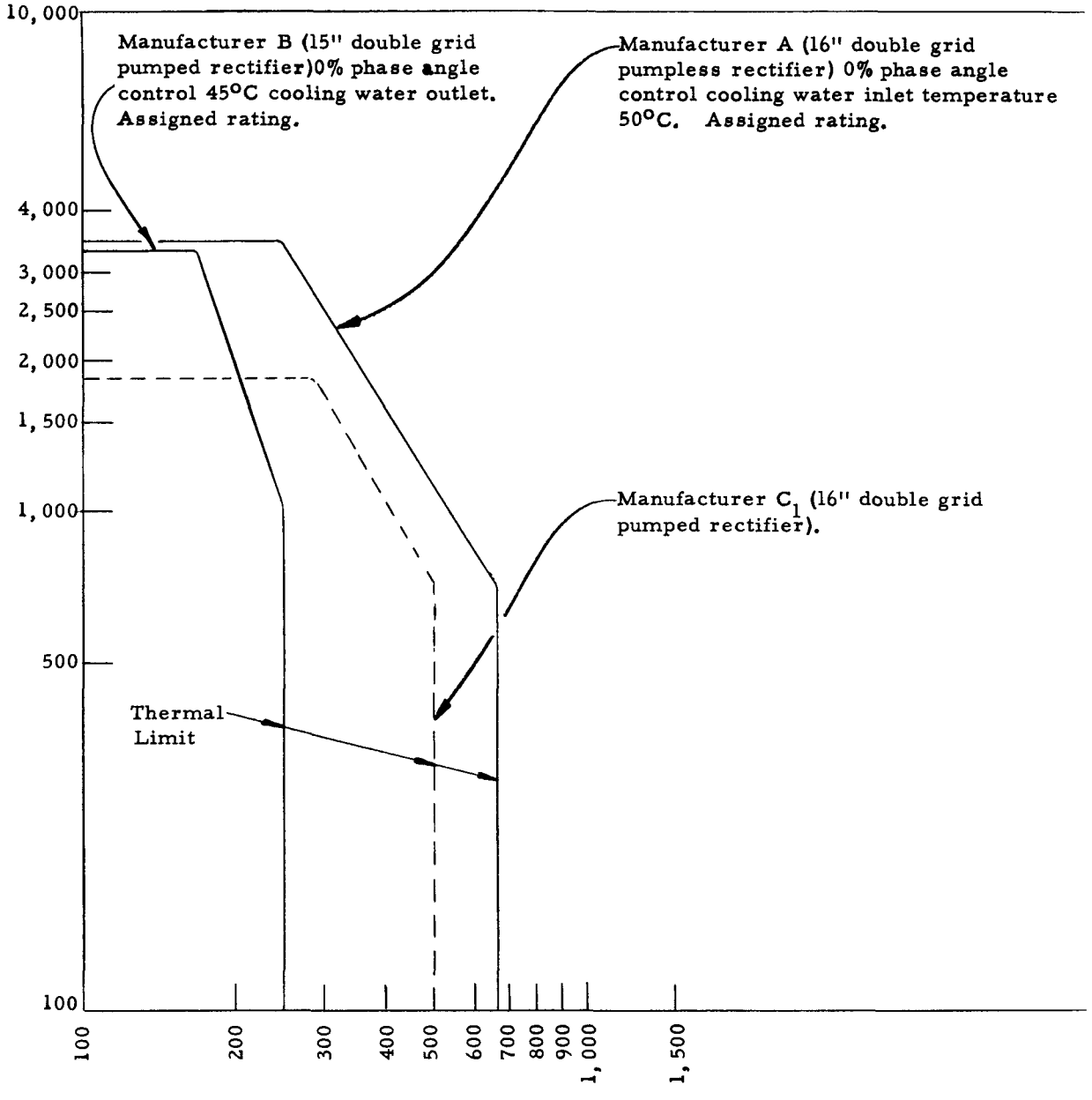
10,000
4,000
3,000
2,500
2,000
1,500
1,000
500
100
Manufacturer B (15" double grid pumped rectifier)0% phase angle control 45°C cooling water outlet. Assigned rating.
Manufacturer A (16" double grid pumpless rectifier) 0% phase angle control cooling water inlet temperature 50°C. Assigned rating.
Manufacturer C1 (16" double grid pumped rectifier).
Thermal Limit
100
200
300
400
500
600
700
800
900
1,000
1,500
Anode Current Average Amperes/Tube
(0 % Phase Angle Control)

Figure 9

TABLE I

Comparison of Rectifier Loading for 3 Different Overall 12-Phase Connections of the Rectifiers Supplying the Ring Magnet of the ZGS, Assuming Zero-Phase Angle Control in All Cases

Rectifier Connections[1]	V, kv	V_1, v	I_m, amp	I_{1m}, amp	I_{av}, amp	I_{rms}, amp	I_r, amp			I_{1av} amp	I_{1av} $\%I_r$			I_{1rms}, amp
							*	⊛	**		*	⊛	**	
($\Delta t = 0$)		(2)												
a)	12 5	1562 1100	10950	2738	2738	4471	415 510	216 245		228	55 00 44 50			373
b)	12 5	3125 2200	10950	1369	2738	4471	265 335	172 195		114		66 30 58 50		186
c)	12 5	1562 1100	10950	2738	2738	4471	415 510	216 245		228	55 00 44 50	105 60 93 10		373
c_1)	12 5	1562 1100	10950	1830	2738	4471			320 390	152			47 50 39 00	248
($\Delta t = 0$ 2 sec)[3]														
a)	12 5	1562 1100	10950	2738	3285	5096	415 510	216 245		274	66 00 53 70			425
b)	12 5	3125 2200	10950	1369	3285	5096	265 335	170 195		137		80 60 70 30		212
c)	12 5	1562 1100	10950	2738	3285	5096	415 510	216 245		274	66 00 53 70	127 00 112 00		425
c_1)	12 5	1562 1100	10950	1830	3285	5096			320 390	183			57 20 47 00	283

NOTES

(1) a) Double way rectification (Fig 6), b) One way rectification (Fig 7), c) Two 6-phase single-way banks connected in cascade (Fig 8), c_1) Same as c except that excitrons are used

(2) Upper and lower figures represent, respectively, the voltage at the beginning and at the end of the rising period

* Based on 96 rectifier tubes each having the voltage vs current ratings of the 16-in rectifiers contemplated by manufacturer A, with zero phase-angle control and 50°C cooling water inlet temperature

⊛ Based on 96 rectifier tubes each having the voltage vs current ratings of the 15-in rectifiers contemplated by manufacturer B, with zero phase-angle control and 45°C cooling water outlet temperature

** Based on 144 rectifier tubes each having the voltage vs current ratings of the 16-in rectifiers contemplated by manufacturer C_1

(3) The voltage V_1 during flat topping will be smaller than either of the figures shown and the corresponding values of I_r greater, so that the % I_r shown are somewhat pessimistic values

V - Total Voltage across Magnet

V_1 - Voltage across Each Rectifier Tube

I_m - Total Peak Current in the Magnet

I_{av} - Total Average Current of the Magnet over the Pulse Duration T

I_{rms} - Root Mean Square Value of the Magnet Current over the Pulse Duration T

I_{1av}, I_{1rms}, I_{1m} - The Corresponding Currents for Each Rectifier Tube

I_r - Assigned Rated Average Current at the Voltage V_1

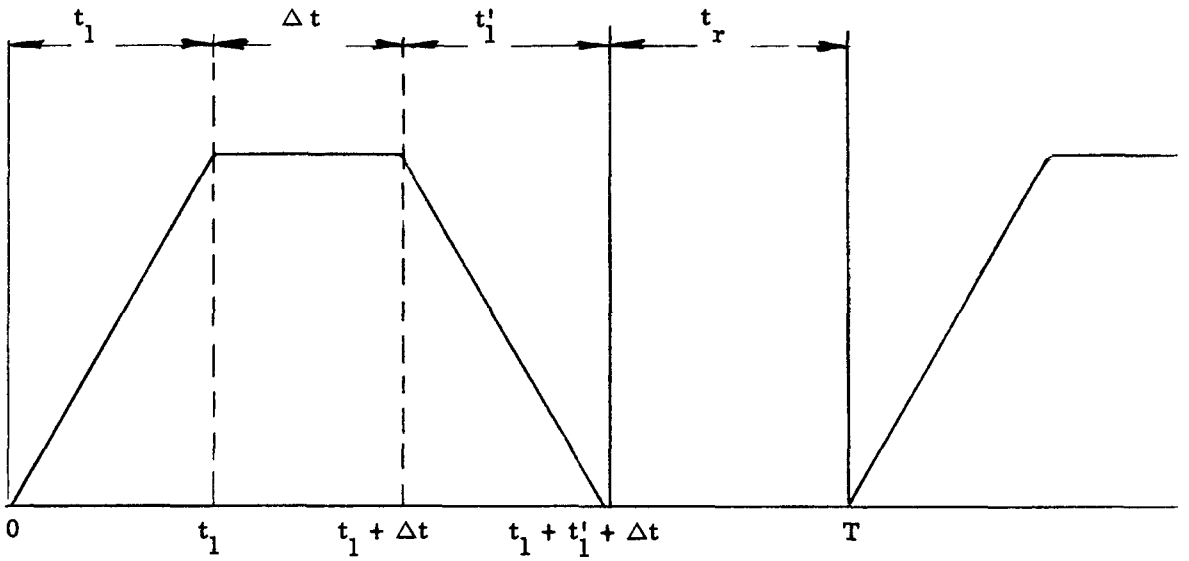

Figure 10

TABLE II

Data on Rectifiers of Some Existing or Projected Accelerators

Accelerator	Number of Feeding Points	Method of Supply at Each Feeding Point	Number of Rectifiers			Type of Rectifiers	
			per Phase	per Feeding Point	Total	Manufacturer	Type
Bevatron	2	1 12-phase generator Rectifiers in series-parallel combination	2	24	48	Westinghouse	IPJ-7
Cosmotron	1	1 12-phase generator with 4 Y windings Rectifiers in series parallel combination	2	24	24	Westinghouse	IPJ-7
AGS	1		2	24	24	Westinghouse	IPJ-7
Harwell	2	8 simple 3-phase rectifiers in parallel These in series with 8 more simple 3-phase rectifiers also in parallel	1	48	96	Brown-Boveri	
CERN	1	2 simple 3-phase rectifiers in parallel These are in series with 2 more simple 3-phase rectifiers also in parallel.	2	24	24	Brown-Boveri	
ZGS	4	Possible alternatives as shown in Figs 6, 7 and 8	2	24	96	Manufacturers A and B	
		Alternative as shown in Fig 8	3	36	144	Manufacturer C_1	

VII. RADIO-FREQUENCY SYSTEM

R. Daniels, H. Kampf, C. Laverick, J. H. Martin, C. Turner, J. Simanton, R. Rothe

A. Accelerating Cavity

To develop confidence in magnetic measurements made on the cavity ferrite frames, preliminary electromagnetic measurements were made on the model RF cavity prior to the insertion of any ferrite. No resonances were found other than the expected fundamental resonance at 4.5 Mc/sec.

The introduction of two frames of Philips ferrite type IV-L1, which is similar to type IV-B, reduced the Q of the model cavity from 1500 to 25 and increased the inductance from 0.085 μh to 1.1 μh. The measured magnetic properties of the ferrite, together with the ferrite specifications, are tabulated below:

MAGNETIC PROPERTIES OF PHILIPS IV-L1 FERRITE

Property	Symbol	Specifications	Measurement
Initial Permeability	μ_i	250	310
Q Value	Q	20	25
Quality Product	$Q\mu f$	10^4	3×10^4
Dielectric Constant	k_e	20	15

Although measurements are not completed, investigations to date indicate that the ferrite permeability will decrease the required amount by the bias field allowed in the specifications.

B. Accelerating Cavity Design

The insulating material for the accelerating gap in the cavity has been chosen to be alumina ceramic type 4462 to be made by Frenchtown Porcelain Co. The present design provides a gap 3 in. wide. The rectangular structure is to be fabricated by bonding together four straight bars of the material. Attachment is to be made by a number of tension studs patted into the frame faces. Delivery of the first assembled frame is expected about July 15, 1959.

C. Radio-frequency Program

Two test systems, which are capable of producing a frequency sweep of from 4.4 to 14 Mc/sec at an amplitude of 1 v ± 20% for voltage ramps of various slopes, maximum amplitudes and repetition frequencies,

have been produced. These systems also incorporate manual control of the frequency sweep and will serve as models for the prototype programming system which is now being designed. The frequency program obtained with these systems is not the same as that required in the final system but suffices for test purposes. High bias fields are used in the tank-circuit ferrites and these are obtained by using bias windings of approximately 100 turns with bias currents of the order of 21 amp. Frequency correction can be applied to these programs from bias generators which control the voltages applied to the voltage-sensitive variable capacitors which are incorporated in the oscillator tank circuit.

The ferrite toroids in the oscillator tank circuit together with their associated bias windings are controlled with regard to temperature by means of a closed-loop temperature-control system which utilizes Silicon 200 fluid as the circulating medium and water-cooled tubes in the heat exchanger. Since the associated voltage-variable capacitors merely have been screened from drafts and are not temperature controlled, the systems cannot be considered as having the degree of temperature stability which will be required in the prototype; for that reason they will not be subjected to the exhaustive tests which a prototype system would have to undergo, but will be used as auxiliary systems in other parts of the RF test and development program.

Stable integrators incorporating Kin Tel operational, DC amplifiers, precision components, temperature control and associated high-speed diode switches have been developed and are at present undergoing tests to determine their suitability for the prototype system.

The prototype programming system will incorporate a diode correction generator, and work on the design of a suitable generator has commenced.

D. Cavity Bias

A bias-current generator incorporating a water-cooled bank of 86 transistors in the output stage and capable of producing a bias current ramp of from 0 to 215 amp in 1 sec, into a load of 0.16 ohm, has been designed and built. The bias current will be programmed so as to provide coarse tuning for the ferrite over the frequency program, the fine tuning being provided by the power amplifier phase-control loop. This bias-current program will be obtained by applying a suitably programmed input voltage to the current generator, the input voltage being derived from a diode function generator whose input voltage ramp will be obtained from the integrated $\dot{B}$ signal. A suitable diode function generator is being developed for this purpose and a test model has already been built.

E. Power Amplifier

All of the power supplies and electronic protection circuits for the full-power prototype amplifier have been completed and tested.

The two broadband coupling transformers required by the amplifier design have proved to be unavailable and will have to be constructed at ANL. The smaller one has been completed and all tests to date indicate that it will perform as required. The tests also indicate the feasibility of the design for the larger one and materials for it are on order.

The design of the interlock and control phases required by the power amplifier has been started and, as soon as full-power tests of the amplifier are successfully completed, the final design of the entire amplifier as used in the synchrotron will be begun.

F. Beam-handling Electrodes

Induction electrode systems are being developed to measure the following beam parameters:

1. the total charge and azimuthal charge distribution in the bunches of accelerated protons;
2. the average radial position of the bunches;
3. the average vertical position of the bunches;
4. the radial width of the bunches; and
5. the vertical width of the bunches.

The induction electrode systems are being developed by means of models in which a charged conducting wire (0.002-in. diameter) is being used to represent a thin beam of charged protons. To simulate a thin beam, the wire should have a line charge density which is as uniform as possible. Measurements have been taken and information has been accumulated on the geometric conditions under which a wire will simulate a thin charged beam. To check the characteristics of experimental electrode systems, it is necessary to:

1. check that the line charge density on the wire is sufficiently uniform within that region of the electrode system which is to be occupied by the synchrotron beam;
2. in addition, it is necessary to check that the electrode system has sufficiently correct radial and vertical characteristics with respect to the position of the calibrating wire.

A fifth experimental model of the induction electrode system to measure the average radial position of the bunches is being tested, and its geometry is expected to closely approximate that of the final model.

The presently planned overall mutually perpendicular dimensions are: azimuth, 30 in.; radially, 48 in.; and vertically, 30 in.

VIII. INJECTION SYSTEM

R. Castor, D. Cohen, P. Livdahl, W. Myers, R. Perry

A. 800-kv Power Supply

Proposals for building an 800-kv DC power supply have been received from several manufacturers. Selection of the system which best meets the specification requirements has been made, and an order for the power supply will go out as soon as the contractual details are completed.

Specifications for the power supply include the following:

Output Voltage	800 kv
Rated Current of Cascade Generator	8 mamp
Stability of Output Voltage, including effects of ripple and of pulsed load of 150 mamp	± 0.1%
Power available in High-voltage Terminal	15 kw

B. Linac Tank

Specifications and design drawings for the Linac tank are nearly completed, and solicitation for bids on fabrication of the tank will go out about July 1.

The tank will be fabricated from 1-in. thick copper-clad steel, will have a diameter of 37.4 in. and a length of 109.2 ft. (The clad steel has been rolled and is ready for fabrication.) It will be made in eleven sections, which will be joined together by means of bolting flanges to make a single RF resonant cavity to operate at 200 Mc/sec.

A vacuum pump port is provided in each tank section to accommodate a 20-in. pump. Provision is also made to connect a 9-in. coaxial line to either of two ports in the middle tank section so that RF power may be fed in at a side or a bottom position.

C. Linac Drift Tubes

Prototypes of representative drift tubes and quadrupole magnets are being made to test all aspects of their fabrication and assembly before production of the final units is undertaken.

Mock-up tests have also been made to verify the feasibility of installing (or removing) assembled drift tubes in the Linac tank.

D. Injector Building

Design requirements for the Injector Building and building services have been submitted to the architect-engineer. Preliminary (Title I) work on the building foundations and structural design has completed by the architect-engineer and approved.

The building will have a basement which will accommodate most of the auxiliary equipment for the injector system and some of the synchrotron RF equipment. In addition, control cable trays from the control building to the synchrotron will be routed through this region.

There will be provision for a radiation shield wall between the Linac and the remainder of the equipment to be located on the main floor. This will permit work on the RF power equipment while the Linac is in operation.

The preaccelerator will be housed in a metal-lined enclosure which will extend from the basement floor to a suitable height above the main floor. Both the preaccelerator area and the Linac section will be served by a 10-ton bridge crane.

The Linac will be supported on caissons which rest on bedrock and which will be isolated from the building foundation.

E. Linac RF System

A purchase order for the Linac RF system has been awarded to the Continental Electronics Manufacturing Company of Dallas, Texas. Specifications for the system are generally outlined in the last Particle Accelerator Division Summary Report (ANL-5956). A block diagram of the entire system is shown in Fig. 11.

The system will be a driven amplifier using a single RCA type A2346F tube as the final amplifier stage, with a power output capability of 5 megawatts at a 500-μsec pulse length and a maximum repetition rate of 10 pulses/sec. This tube has demonstrated a capability greater than this, both on peak power and average power bases, in other applications. It is expected that a plate voltage pulse of 35 kv and 250 amp will be required to develop the full-power output from the A2346F.

The modulator will utilize four Machlett 5682 tubes in series-parallel as switch tubes. Each set of paralleled 5682's will be placed on an insulated deck with their associated drivers, bias and filament supplies. Primary power for bias and filament supplies will be furnished from

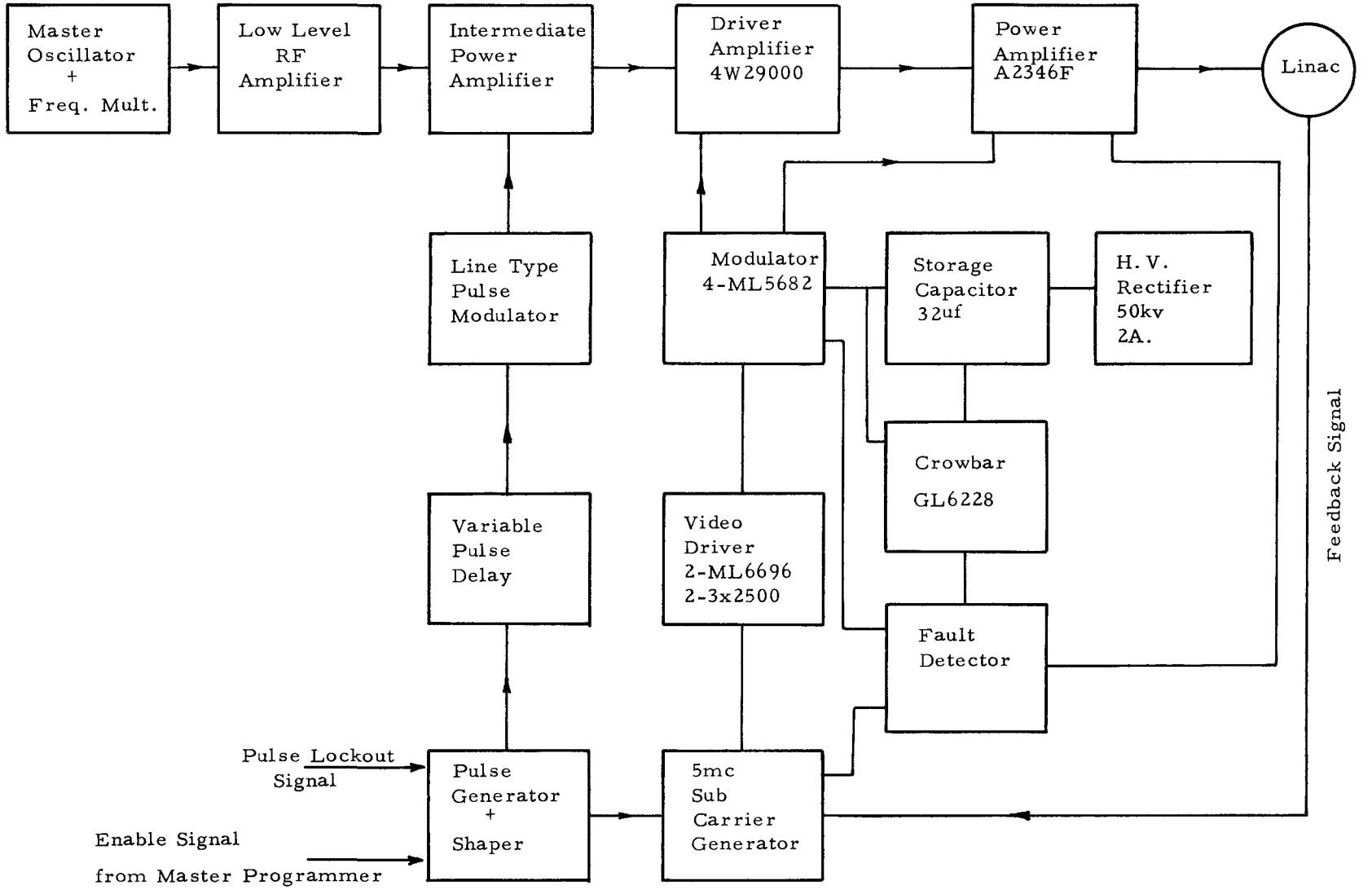

Linac RF System Block Diagram

Figure 11

isolation transformers to each modulator deck. The modulator tubes will also serve as series voltage regulators during the pulse to control the modulator for either constant plate voltage to the final amplifier or by changing the source of the regulating signal, constant RF voltage in the Linac cavity. Control of the modulator is derived from a 5-Mcps oscillator which is coupled through RF transformers to each deck. The amplitude of the 5-Mc signal determines the voltage drop across each modulator deck by determining the grid bias on the 5682's. Lack of a 5-Mc signal will automatically cut off the modulator tubes.

Primary protection for the system will be derived by interrupting the pulse to the final amplifier by cutting off the modulator switch tubes. In the event of a fault in the modulator itself, a crowbar is provided which will short the high voltage to ground until the overload breakers in the primary of the high-voltage changing supply can operate. Fault-sensing devices will be supplied in the cathode lead of each modulator tube as well as the cathode lead of the final amplifier.

Low-level stages of the amplifier will be CW. The intermediate stage will be plate pulsed by its own line-type modulator whose trigger may be delayed by a variable delay line, so that drive to the final stage may be applied after the plate voltage is at its maximum value in order to have the fastest possible RF rise time out of the final amplifier.

Testing of the low-level and intermediate-level amplifier, as well as of pulse control and modulator control circuits, has begun. Testing of the complete system is scheduled to begin by November 1959 with delivery by August 15, 1960.

F. Ion Source and Preaccelerator

Assembly of the test facility for ion source and accelerating column testing has been completed and all voltages of the component tested. The isolation transformer was found to be unsatisfactory and the supplier has redesigned the unit. They will deliver a new transformer by August 1; meanwhile, the original unit is being used at a voltage below the design of 300 kv.

Auxiliary equipment for operation of the CERN type, ceramic RF source has been built and tested. Coupling of sufficient amounts of RF power into the source together with high extraction voltages has been troublesome and as yet the results of the CERN group have not been duplicated.

Assembly of the short accelerating column described in ANLAD-53 is complete and testing of this configuration has been started.

G. Linac Vacuum System

The preliminary design of the vacuum system has been completed and a study of component parts is now underway. The Linac cavity will be furnished with 10-20-in. mercury diffusion pumps which will be baffled with mechanically refrigerated baffles. The preaccelerator section and debuncher section of the system will be furnished with 10-in. mercury diffusion pumps at six pumping stations along the beam tube.

IX. THEORETICAL STUDIES ON RADIAL MOTIONS THROUGH THE LINEAR ACCELERATOR

D. Cohen

Further use was made of the nonlinear IBM-704 computing program for tracing radial motions through the Linac. Some 20 cases of random quadrupole rotational misalignments with a maximum of ±0.11° were run for both ++-- and +-+- modes, and the average amplitude growth was about 2%. It may be concluded that the allowable upper limit for rotational misalignments can be relaxed from the previous working number of ±10 minutes of arc to ±25 minutes of arc.

The effects of magnet ripple were investigated by assuming that various groups of magnets experienced the same ripple, and examining the Linac acceptance figures as a function of ripple amplitude and grouping. It was found that a peak-to-peak ripple of 5% produced no significant disturbance of the acceptance figures. Under conditions where eight or more consecutive magnets have gradients which deviate as a group from the ideal program, disturbances are not easily induced. If every other two magnets (in ++--) or every other magnet (in +-+-) is allowed to deviate, then predictably significant effects are encountered.

The study of Linac acceptance and emittance figures in phase space, and the behavior of these figures with respect to beam matching to the synchrotron, led to consideration of the synchrotron acceptance. Rearrangement of previously calculated results by Teng and Crosbie indicated that for injection purposes the synchrotron acceptance quality for vertical motion should be considered to be something greater than 1.2 milliradian-inches. This is about twice the Linac output quality in the +-+- mode, so that certain restrictions of Linac operation and beam-matching equipment which normally exist with critical matching may be removed. This last statement assumes the Linac phase space is largely filled by the source and column; if the populated area is small, then the restrictions do not exist in the first place.

Auxiliary Calculations

A. Heating Method for Measuring Radio-frequency Gradients

A proposed method for measuring the electric field magnitudes between drift tubes by observing the infrared radiation from a field-heated object has been investigated. It was hoped that the fields might be measured with greater precision than allowed with the "globall" method. However, it was deduced eventually that only borderline success could be attained, and this only with painstaking and elaborate experimental care and complexity.

B. The Effect of the Linac on a Polarized Beam

Because the use of the ZGS would be greatly enhanced if polarized beams of protons could be produced, calculations were begun to see if the Linac, as a separate entity, would accelerate a source-polarized beam without undue depolarization. No definite information is available at present on the effect on a polarized beam of the rest of the accelerating and beam-handling complex. Preliminary Linac results, using the orbits previously calculated with the IBM-704, indicate that in the ++-- mode the magnetic moments do not change their direction by more than 10° in passing through the Linac. Orbits calculated up to now are: pure horizontal and pure vertical oscillations, of largest amplitude, with initial angles and initial displacements. The more tedious case of mixed horizontal and vertical oscillations is yet to be performed; one guesses that the depolarization in this general case will also be small.

X. MISCELLANEOUS

F. W. Markley, R. D. Roman

Plastics

A. Outgassing of Plastics, Elastomers, and Metals (Measurements by R. Vosecek)

The outgassing measurements previously described in reports ANL-5864 and ANL-5956 have been continued and extended. It was stated in these earlier reports that some error in our measurements resulted from an unexpected pumping action in the closed test chamber. It was assumed that this pumping was due to the ionization gauge. It is now known that this error is not large, due to the saturation of the pumping action as the chamber pressure increases. Figure 12 shows the effect of ionization gauge pumping, illustrating gauge saturation. Each curve was obtained by taking a series of slopes to the curve of pressure vs time for the closed chamber containing the sample. Each curve differs from the others only in the starting pressure of the run. Sample outgassing should decrease with increasing pressure, but the saturation effect causes the ion gauge pumping to decrease with increasing pressure also. Therefore, the sum of these two effects, i.e., the measured outgassing, may vary directly or inversely with pressure according to their relative magnitudes. For the curves with very low starting pressures, the ion gauge pumping is initially almost as large as the sample outgassing, and as the gauge saturates the pumping is reduced faster than the sample outgassing, yielding a measured outgassing rate that increases with pressure. For the curves with high starting pressures, the ion gauge pumping is always considerably less than sample outgassing, so that the normal inverse relationship between measured outgassing and pressure is seen. All curves reach the same value at 10^{-3} mm Hg, indicating complete gauge saturation and consequently no further pumping. Therefore, our measurements, taken at 5×10^{-4} mm Hg, may be seen to be little affected by ion gauge pumping.

Figure 13 shows the comparative outgassing of the various materials tested at this Laboratory. These curves are intended for comparison only. They do not show the details of the experimental data, and in most cases are only linear approximations to the original data points. The actual data are available on request. The outgassing shown was measured on samples of approximately 40-cm^2 area at a pressure of 5×10^{-4} mm Hg. The samples received no special conditioning. The direct ion gauge readings were used (calibrated for air). No attempt has yet been made to correct the ion gauge for the actual gas evolved from the samples. However, this is now possible with fair certainty since Prosser and Turnbull at Harwell, England (AERE C/M 362), have run a mass spectrometric analysis on three epoxy samples and found water vapor to be the only gas evolved in detectable amounts.

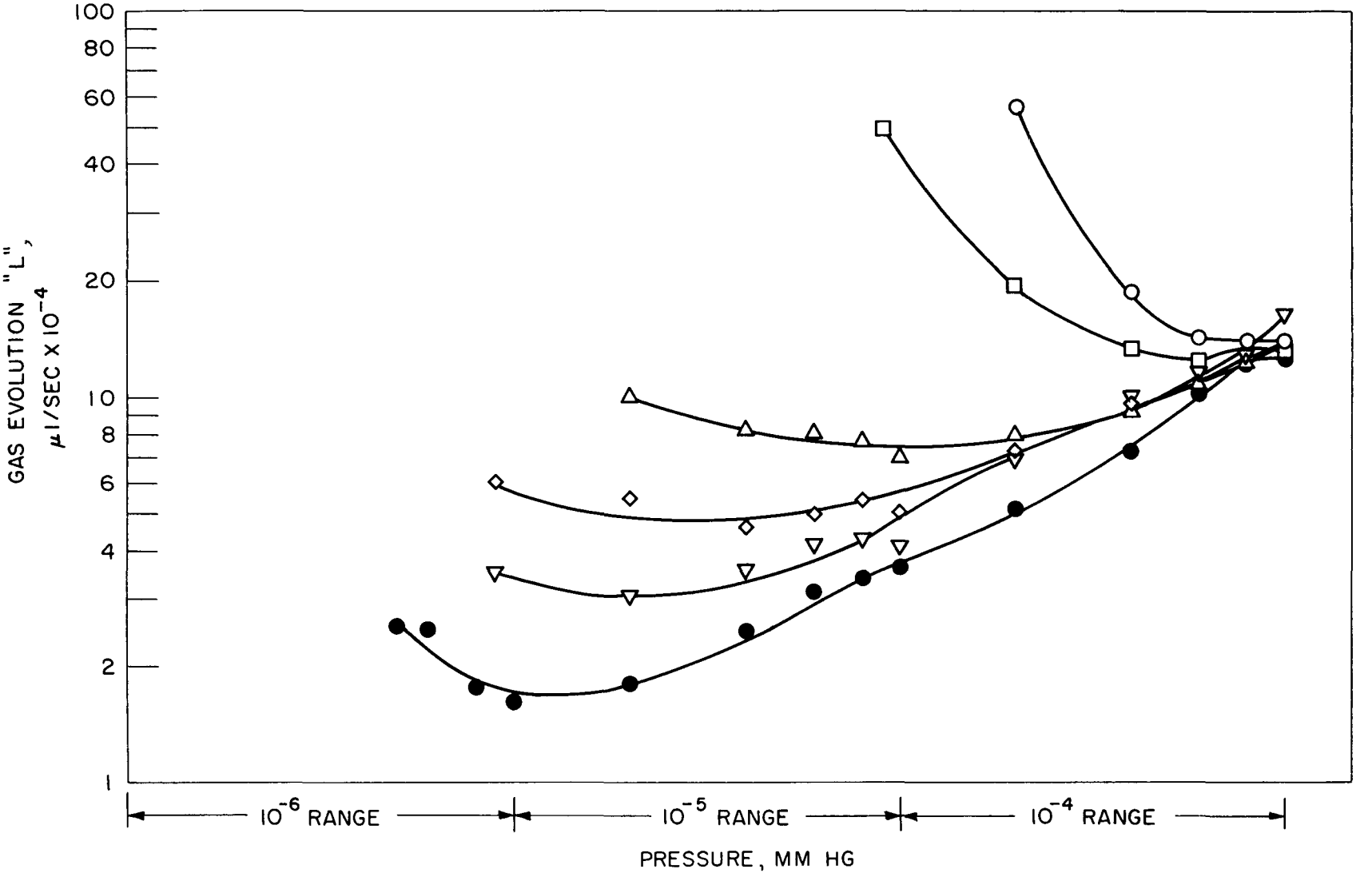

EFFECT OF IONIZATION GAUGE PUMPING ILLUSTRATING GAUGE SATURATION
TEST SAMPLE 1001-PA
FIGURE 12

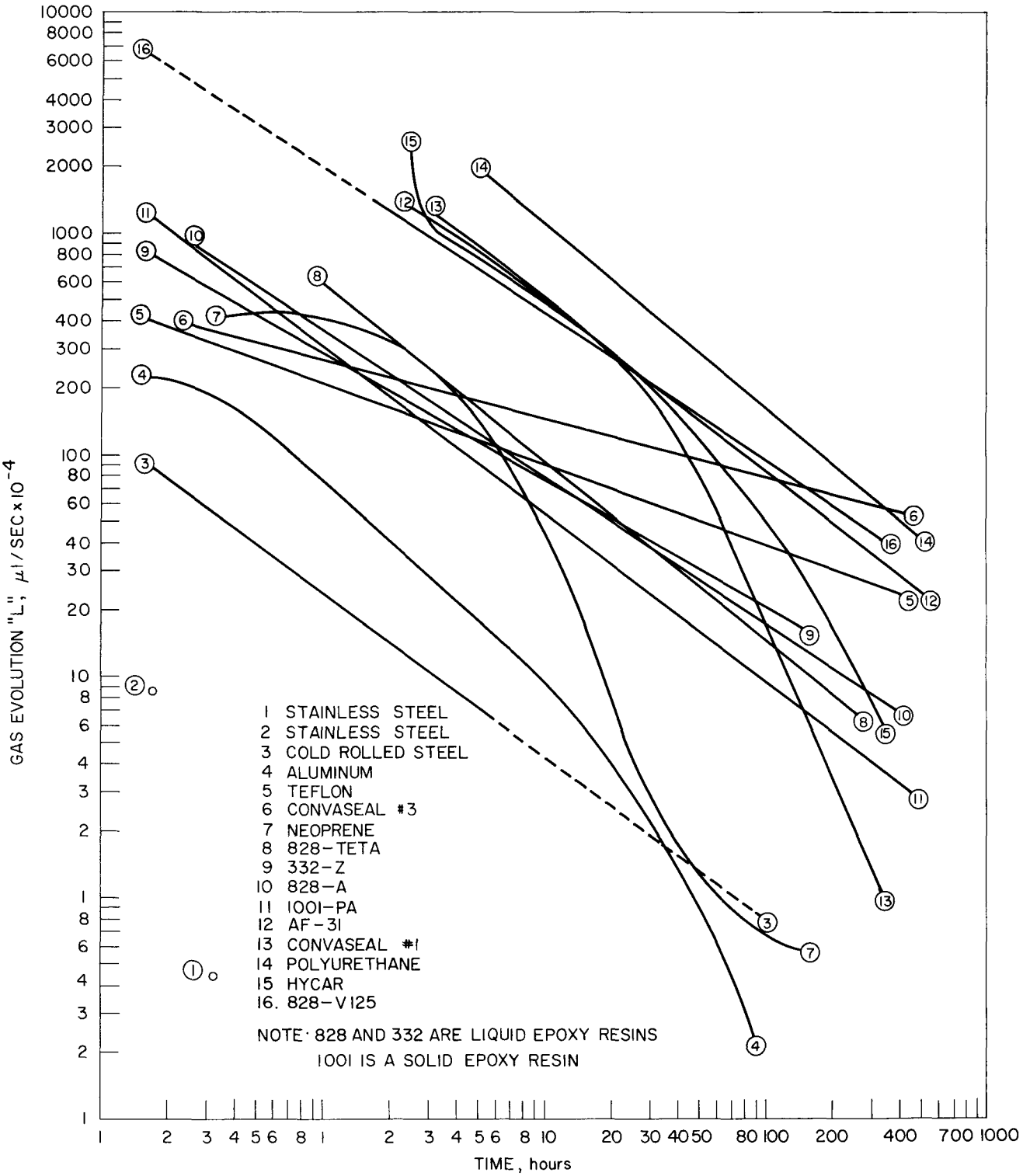

COMPARATIVE OUTGASSING OF VARIOUS MATERIALS

FIGURE 13

This new information showing the ion gauge pumping to be small at 5×10^{-4} mm Hg and the vapor evolved from epoxies to be water means that it is not vitally important that we have not succeeded in using the Knudsen gauge, mentioned in the last report, with our apparatus. We would still like to incorporate this gauge into our test apparatus, particularly with a view to measuring outgassing rates at lower pressures directly instead of trying to calculate them from the values obtained at 5×10^{-4} mm Hg.

In the immediate future our efforts will be concentrated on obtaining a complete picture of the outgassing from Minnesota Mining and Manufacturing Company's nitrile-phenolic tape, Scotchply No. AF-31. From the mechanical and construction view point, this tape looks like the most promising material for the construction of the inner high-vacuum chamber.

B. Ferrite Bonding

Summary report ANL-5864 mentioned that a bonding system had been perfected for assembly of the ferrite frames in the RF cavity. The design of the ferrite frames has since been changed by the RF group, requiring the development of a new bonding system. The requirement of this new system is not high bond strength, but high thermal conductivity. A guarded ring hot plate apparatus to measure thermal conductivity has been built and is now in use. The conductivity of a pure epoxy bonding agent proposed as base resin for this job is found to be 3.7×10^{-4} cal/sec/cm^2/°C/cm. Loading this resin with 74% by weight of copper gives a value 18.3×10^{-4}. Loading with 65% quartz powder by weight gives a value of 18.3×10^{-4} also. These mixtures had approximately equal viscosities. The calculated values of thermal conductivity to be expected for these samples if a series thermal connection is assumed for plastic and filler are 5.1×10^{-4} and 6.7×10^{-4}.

These measured values of thermal conductivity are still smaller than we desire. They may be improved by higher filler loading, increased filler particle size (this would add some additional parallel thermal connections), and vacuum mixing to eliminate entrapped air. However, we are also investigating a commercial material, Emerson and Cummings Eccobond 60-L. The electrical conductivity of 50 ohm-cm given by the manufacturer would indicate excellent thermal conductivity, and the price is not unreasonable. We have not yet measured its actual thermal conductivity, as a preliminary electrical check shows that vacuum mixing is required to reach the properties given by the manufacturer. A vacuum mixing machine is on order and should be delivered soon. A satisfactory solution to this problem should be reached in the near future.

C. General

Within the past year, the activities of the plastics section have rapidly expanded to include not only primary engineering design and development, but also a wide variety of service and consultation functions for other groups within the Division. These include special material fabrication, special equipment design and construction, and plastics and adhesives problems, research and consultation. The heavy workload in this area indicates the importance of the versatile synthetic organic materials in the physics research and development work of today. Very substantial savings in the cost and in construction time of special equipment have been effected through the availability of these services. In some cases, special apparatus would have been impractical or even impossible to build without these services.